Trotter-Based Simulation of Quantum-Classical Dynamics†

Dónal Mac Kernan,* Giovanni Ciccotti, and Raymond Kapral

School of Physics, Trinity College Dublin, Dublin 2 and School of Physics, University College Dublin, Dublin 4, Ireland, INFM and Dipartimento di Fisica, Università "La Sapienza", Piazzale Aldo Moro, 2, 00185 Roma, Italy, and Chemical Physics Theory Group, Department of Chemistry, University of Toronto, Toronto, ON M5S 3H6, Canada

Received: August 1, 2007; In Final Form: October 11, 2007

Quantum rate processes in condensed phase systems are often computed by combining quantum and classical descriptions of the dynamics. An algorithm for simulating the quantum-classical Liouville equation, which describes the dynamics of a quantum subsystem coupled to a classical bath, is presented in this paper. The algorithm is based on a Trotter decomposition of the quantum-classical propagator, in conjunction with Monte Carlo sampling of quantum transitions, to yield a surface-hopping representation of the dynamics. An expression for the nonadiabatic propagator that is responsible for quantum transitions and associated bath momentum changes is derived in a form that is convenient for Monte Carlo sampling and exactly conserves the total energy of the system in individual trajectories. The expectation values of operators or quantum correlation functions can be evaluated by initial sampling of quantum states and use of quantum-classical Liouville dynamics for the time evolution. The algorithm is tested by calculations on the spin-boson model, for which exact quantum results are available, and is shown to reproduce the exact results for stronger nonadiabatic coupling and much longer times using fewer trajectories than other schemes for simulating quantum-classical Liouville dynamics.

1. Introduction

An understanding of the dynamical properties of condensed phase quantum systems underlies the description of a variety of quantum phenomena in chemical and biological systems. These phenomena include, among others, nonadiabatic chemical rate processes involving electronic, vibrational, or other degrees of freedom, decoherence in open quantum systems, and quantum transport processes. Quantum effects underlie the study of ultrafast rate processes in solution.[1,2] The development of schemes for the efficient and accurate simulation of the quantum dynamics of such systems is an active area of research in chemical physics[3−15] and is essential if problems of chemical interest involving complex molecular species in the condensed phase are considered. This article is concerned with the development of such a simulation method.

In investigations of the dynamical properties of quantum statistical mechanical systems, one is often interested in the average value of some operator when the system evolves from a given initially prepared distribution described by the density matrix $\hat{\rho}(0)$. In such cases, the quantum mechanical average value of an operator $\hat{B}$ is given by

$$\overline{B(t)} = \mathrm{Tr}\hat{B}\hat{\rho}(t) = \mathrm{Tr}\hat{B}(t)\hat{\rho}(0) \tag{1}$$

In the last equality $\hat{B}(t)$ evolves in time through the Heisenberg equation of motion, $\mathrm{d}\hat{B}(t)/\mathrm{d}t = (i/\hbar)[\hat{H},\hat{B}(t)]$, where $\hat{H}$ is the Hamiltonian operator. Alternatively, one may be interested in the calculation of a transport property λ, which may generally be written as a time integral of a quantum mechanical correlation function of two operators $\hat{A}$ and $\hat{B}$,

$$\lambda \sim \int_0^\infty \mathrm{d}t\ \mathrm{Tr}\hat{B}(t)\hat{A}\hat{\rho}_{\mathrm{eq}} \equiv \int_0^\infty \mathrm{d}t\ \langle \hat{B}(t)\hat{A}\rangle \tag{2}$$

where $\hat{\rho}_{\mathrm{eq}} = \mathrm{e}^{-\beta\hat{H}}/\mathrm{Tr}\ \mathrm{e}^{-\beta\hat{H}}$ is the canonical equilibrium density matrix. The computation of either of these expressions involves averages over initial quantum distributions and time evolution of a quantum operator.

In many applications, it is useful to partition the system into a subsystem and a bath. A phase space description of the bath can be obtained by taking a partial Wigner transform over the bath coordinate $\{Q\}$ representation of the full quantum system.[17,18] The partial Wigner transform of an operator $\hat{B}$ is defined as[19]

$$\hat{B}_W(R,P) = \int \mathrm{d}z\ \mathrm{e}^{iP\cdot z/\hbar}\left\langle R - \frac{z}{2}\middle|\hat{B}\middle|R + \frac{z}{2}\right\rangle \tag{3}$$

with an analogous definition for the partial Wigner transform of the density matrix. Thus, $\hat{B}_W(R,P)$ is an abstract operator in the vector space of the subsystem and depends on the phase space variables (R, P) of the bath. In this partial Wigner representation, the expectation value of $\hat{B}(t)$ takes the form

$$\overline{B(t)} = \mathrm{Tr}' \int \mathrm{d}R\ \mathrm{d}P\ \hat{B}_W(R,P,t)\hat{\rho}_W(R,P) \tag{4}$$

where the prime on the trace indicates a trace over the subsystem degrees of freedom and $\hat{\rho}_W(R,P) \equiv \hat{\rho}_W(R,P,0)$. All information on the quantum initial distribution is contained in $\hat{\rho}_W(R,P,0)$. Similarly, in the partial Wigner representation, a transport property takes the form[17,20,21]

$$\lambda \sim \int_0^\infty \mathrm{d}t\ \mathrm{Tr}' \int \mathrm{d}R\ \mathrm{d}P\ \hat{B}_W(R,P,t)(\hat{A}\hat{\rho}_{\mathrm{eq}})_W(R,P) \tag{5}$$

† Part of the "James T. (Casey) Hynes Festschrift".

* Corresponding author.

10.1021/jp0761416 CCC: $40.75
Published on Web 12/22/2007

where initial quantum correlations are described by $(\hat{A}\hat{\rho}_{eq})_W(R, P)$. In both cases, the quantum evolution of the dynamical variable must be computed to obtain the expectation value or transport property. These quantum statistical mechanical expressions are exact. In this partial Wigner representation, the computation of the full quantum evolution of $\hat{B}_W(R, P, t)$ for a large many-body system is still an intractable problem. Because of the difficulty of simulating the quantum dynamics of large many-body systems, most quantum dynamics methods, for example, surface-hopping schemes,[22,16] consider the combined evolution of quantum and classical degrees of freedom.

Given this perspective, we consider systems whose dynamics may be accurately approximated by quantum-classical Liouville equation.[17,23] This is the case, for instance, if the subsystem and bath consist of particles with masses m and M, respectively, and $m \ll M$.[18] Furthermore, if the bath is harmonic and bilinearly coupled to the subsystem, then quantum-classical Liouville dynamics entails no approximation and is equivalent to a full quantum description of the dynamics of the entire system.[24] The quantum-classical Liouville equation for an observable is[18]

$$\frac{d\hat{B}_W(t)}{dt} = \frac{i}{\hbar}[\hat{H}_W, \hat{B}_W(t)] - \frac{1}{2}(\{\hat{H}_W, \hat{B}_W(t)\} - \{\hat{B}_W(t), \hat{H}_W\}) \equiv i\hat{\mathscr{L}}\hat{B}_W(t) \quad (6)$$

where the last line defines $\hat{\mathscr{L}}$, the quantum-classical Liouville operator.[18,25−30,10] While the formal solution of this equation of motion is easily written as $\hat{B}_W(t) = \exp(i\hat{\mathscr{L}}t)\hat{B}_W(0)$, the construction of effective simulation algorithms for realistic many-body systems is not a simple task, and a number of different methods have been proposed.[29−34]

In this paper, we describe a Trotter-based scheme for simulating quantum-classical Liouville dynamics in terms of an ensemble of surface-hopping trajectories. The method can be used to compute the dynamics for longer times with fewer trajectories than the sequential short-time propagation (SSTP) algorithm, which is also based on surface-hopping trajectories.[34,35] Section 2 formulates the problem in an adiabatic basis that is convenient for a description of the dynamics in terms of surface-hopping trajectories. The Trotter decomposition of the quantum-classical propagator in a form that conserves energy in nonadiabatic transitions is presented in this section for a two-level system coupled to an arbitrary bath. On the basis of this formulation, the Trotter-based quantum-classical (TBQC) algorithm that is used to simulate the dynamics is described in section 3. The efficacy of the simulation method is illustrated in section 4 where results for the spin-boson model are presented. Since quantum-classical Liouville dynamics is equivalent to full quantum mechanics for this model, comparisons with exact quantum results may be made. Appendices A and B give additional details and sketch the generalization to the multistate case. Although the focus of this paper is on simulation schemes and their application to the standard spin-boson test case, the methods developed here should provide a means to simulate more effectively the quantum dynamics of realistic models of systems of chemical interest.

2. Trotter Factorization of Quantum-Classical Propagator

The evolution of quantum-classical dynamics described by the Liouville operator $\hat{\mathscr{L}}$ may be formulated in terms of an ensemble of surface-hopping trajectories. For this purpose, it is convenient to work in a basis of adiabatic eigenfunctions. The partially Wigner transformed Hamiltonian is the sum of the kinetic energy of the bath particles with mass M, $P^2/2M$, and the subsystem Hamiltonian in the field of the fixed bath particles, $\hat{h}_W(R)$. The total Hamiltonian is given by $\hat{H}_W = P^2/2M + \hat{h}_W(R)$. The adiabatic eigenfunctions $|\alpha; R\rangle$ are the solutions of the eigenvalue problem, $\hat{h}_W(R)|\alpha; R\rangle = E_\alpha(R)|\alpha; R\rangle$. In this basis, the quantum-classical Liouville superoperator has matrix elements (see ref 18 for derivations and full definitions),

$$i\mathscr{L}_{\alpha\alpha',\beta\beta'} = (i\omega_{\alpha\alpha'} + iL_{\alpha\alpha'})\delta_{\alpha\beta}\delta_{\alpha'\beta'} - \mathscr{J}_{\alpha\alpha',\beta\beta'} \equiv i\mathscr{L}^0_{\alpha\alpha'}\delta_{\alpha\beta}\delta_{\alpha'\beta'} - \mathscr{J}_{\alpha\alpha',\beta\beta'} \quad (7)$$

Here, $\omega_{\alpha\alpha'}(R) = (E_\alpha(R) - E_{\alpha'}(R))/\hbar$ and $iL_{\alpha\alpha'}$ is the Liouville operator that describes the classical evolution determined by the mean of the Hellmann−Feynman forces corresponding to adiabatic states α and α',

$$iL_{\alpha\alpha'} = \frac{P}{M}\cdot\frac{\partial}{\partial R} + \frac{1}{2}(F^\alpha_W + F^{\alpha'}_W)\cdot\frac{\partial}{\partial P} \quad (8)$$

where $F^\alpha_W = -\langle\alpha; R|(\partial\hat{H}_W(\hat{q}, R))/\partial R|\alpha; R\rangle$ is the Hellmann−Feynman force for state α. The operator $\mathscr{J}_{\alpha\alpha',\beta\beta'}$ is responsible for nonadiabatic transitions and associated changes in the bath momentum and can be written as the sum of two terms,

$$\mathscr{J}_{\alpha\alpha',\beta\beta'} = J_{1\alpha\alpha',\beta\beta'} + J_{2\alpha\alpha',\beta\beta'} \quad (9)$$

where

$$J_{1\alpha\alpha',\beta\beta'} = -(d_{\alpha\beta}\delta_{\alpha'\beta'} + d^*_{\alpha'\beta'}\delta_{\alpha\beta})\cdot\frac{P}{M} \quad (10)$$

$$J_{2\alpha\alpha',\beta\beta'} = -\frac{1}{2}((E_\alpha - E_\beta)d_{\alpha\beta}\delta_{\alpha'\beta'} + (E_{\alpha'} - E_{\beta'})d^*_{\alpha'\beta'}\delta_{\alpha\beta})\cdot\frac{\partial}{\partial P} \quad (11)$$

and $d_{\alpha\beta}(R) = \langle\alpha; R|\partial/\partial R|\beta; R\rangle$ is the nonadiabatic coupling matrix element. The matrix elements of the quantum-classical propagator in the adiabatic basis are $(\exp(i\mathscr{L}t))_{\alpha\alpha',\beta\beta'}$. The superoperator notation involving pairs of quantum states can be eliminated by associating an index $s = \alpha\mathscr{N} + \alpha'$ with the pair $(\alpha\alpha')$, where $0 \le \alpha,\alpha' < \mathscr{N}$ for an $\mathscr{N}$-state quantum subsystem.[24] The quantum-classical propagator then takes the form $(\exp(i\mathscr{L}t))_{ss'}$ where $i\mathscr{L}_{ss'} = i\mathscr{L}^0_s\delta_{ss'} - \mathscr{J}_{ss'}$.

The starting point of the analysis is similar to that for the SSTP algorithm[34] where the propagator is written as a product of short-time segments. Since the Liouville operator is time independent and commutes with itself we may write the propagator exactly as the product of N short time propagators as

$$(e^{i\mathscr{L}t})_{s_0s_N} = \sum_{s_1s_2\cdots s_{N-1}}\prod_{j=1}^{N}(e^{i\mathscr{L}(t_j - t_{j-1})})_{s_{j-1}s_j} \quad (12)$$

where $t_j = j\delta$ and $t = N\delta$. Moreover, now the propagator for each of the small time intervals $t_j - t_{j-1} = \delta$ is computed by using a Trotter factorization as

$$(e^{i\mathscr{L}(t_j - t_{j-1})})_{s_{j-1}s_j} \approx e^{i\mathscr{L}^0_{s_{j-1}}\delta/2}(e^{-i\mathscr{J}\delta})_{s_{j-1}s_j}e^{i\mathscr{L}^0_{s_j}\delta/2} + \mathscr{O}(\delta^3) \quad (13)$$

where we have used the fact that $i\mathscr{L}^0$ is diagonal in the adiabatic basis. The propagator $e^{i\mathscr{L}_s{}^0(t_j - t_{j-1})}$ can be written as the product of a phase factor and a classical evolution operator as[18]

$$e^{i\mathscr{L}_s^0(t_j-t_{j-1})} = e^{i\int_{t_{j-1}}^{t_j} d\tau\, \omega_s(R_{s,\tau})}\, e^{iL_s(t_j-t_{j-1})} \equiv \mathscr{W}_s'(t_{j-1}, t_j)\, e^{iL_s(t_j-t_{j-1})} \quad (14)$$

where $R_{s,\tau}$ denotes the value of R at time τ obtained by classical evolution under the Hellmann−Feynman force with quantum state index s. The propagator $(e^{-\mathscr{J}\delta})_{ss'}$ is responsible for quantum transitions and bath momentum changes and, henceforth, we refer to it as the nonadiabatic propagator. If the nonadiabatic propagator is set to unity, quantum-classical dynamics reduces to adiabatic dynamics. In order to proceed, we must be able to compute the action of the nonadiabatic propagator on partially Wigner transformed operators.

Nonadiabatic Propagator for a Two-Level System. The structure of $\mathscr{J}$ in eq 9 as the sum of two terms, one of which is a differential operator in the bath momenta, suggests that the evaluation of this propagator can be carried out by a further Trotter decomposition. Here, we show how this term can be evaluated for a two-level system using the momentum-jump approximation[17,18] which is valid to $\mathscr{O}(\delta^2)$. A discussion of the general multi-level case is given in Appendix B.

For a two-level system with states $\alpha = 0, 1$, the index s takes the values from the set $\mathscr{S} = \{0, 1, 2, 3\}$ corresponding to the pairs of state indices (00), (01), (10), and (11), respectively. The matrix operator $\mathscr{J} = J_1 + J_2$ with elements $\mathscr{J}_{ss'} = J_{1,ss'} + J_{2,ss'}$ is a 4×4 matrix. The J_1 matrix has the explicit antisymmetric form,

$$J_1 = \begin{pmatrix} 0 & 1 & 1 & 0 \\ -1 & 0 & 0 & 1 \\ -1 & 0 & 0 & 1 \\ 0 & -1 & -1 & 0 \end{pmatrix} \frac{P}{M} \cdot d_{10}(R) \quad (15)$$

where we have used the fact that $d_{01} = -d_{10}$ for a real adiabatic basis. This matrix may be diagonalized by a matrix V, $J_1V = VD_1$, where D_1 is the diagonal matrix of zero or purely imaginary eigenvalues $\{0,\ 0,\ 2\imath\, P/M\cdot d_{10},\ -2\imath\, P/M\cdot d_{10}\}$. Similarly, the symmetric matrix J_2 has the form,

$$J_2 = -\begin{pmatrix} 0 & 1 & 1 & 0 \\ 1 & 0 & 0 & 1 \\ 1 & 0 & 0 & 1 \\ 0 & 1 & 1 & 0 \end{pmatrix} \frac{1}{2}\hbar\omega_{10}(R)d_{10}(R) \cdot \frac{\partial}{\partial P} \quad (16)$$

It may be diagonalized by a matrix K, $J_2K = KD_2$, where D_2 is a diagonal matrix with eigenvalues $\{-\hbar\omega_{10}(R)d_{10}(R)\cdot\partial/\partial P,\ 0,\ 0,\ \hbar\omega_{10}(R)d_{10}(R)\cdot\partial/\partial P\}$. (The matrices V and K are given in Appendix A.) In order to obtain a form of the short time propagator, we employ a second-order Trotter decomposition of this operator[36] and write

$$e^{-\mathscr{J}\delta} = e^{-J_1\delta}\, e^{-J_2\delta} + \mathscr{O}(\delta^2) = Q_1Q_2 + \mathscr{O}(\delta^2) \quad (17)$$

Here, $Q_1 = e^{-J_1\delta} = V\, e^{-D_1\delta}V^{-1}$ with

$$Q_1 = \begin{pmatrix} \cos^2(a) & -\cos(a)\sin(a) & -\cos(a)\sin(a) & \sin^2(a) \\ \sin(a)\cos(a) & \cos^2(a) & -\sin^2(a) & -\sin(a)\cos(a) \\ \sin(a)\cos(a) & -\sin^2(a) & \cos^2(a) & -\sin(a)\cos(a) \\ \sin^2(a) & \sin(a)\cos(a) & \sin(a)\cos(a) & \cos^2(a) \end{pmatrix} \quad (18)$$

where $a = P/M\cdot d_{10}(R)\delta$. Also, $Q_2 = e^{-J_2\delta} = K\, e^{-D_2\delta}\, K^{-1}$with

$$Q_2 = \frac{1}{2}\begin{pmatrix} 1+\frac{e^{\hat{b}}+e^{-\hat{b}}}{2} & \frac{e^{\hat{b}}-e^{-\hat{b}}}{2} & \frac{e^{\hat{b}}-e^{-\hat{b}}}{2} & -1+\frac{e^{\hat{b}}+e^{-\hat{b}}}{2} \\ \frac{e^{\hat{b}}-e^{-\hat{b}}}{2} & 1+\frac{e^{\hat{b}}+e^{-\hat{b}}}{2} & -1+\frac{e^{\hat{b}}+e^{-\hat{b}}}{2} & \frac{e^{\hat{b}}-e^{-\hat{b}}}{2} \\ \frac{e^{\hat{b}}-e^{-\hat{b}}}{2} & -1+\frac{e^{\hat{b}}+e^{-\hat{b}}}{2} & 1+\frac{e^{\hat{b}}+e^{-\hat{b}}}{2} & \frac{e^{\hat{b}}-e^{-\hat{b}}}{2} \\ -1+\frac{e^{\hat{b}}+e^{-\hat{b}}}{2} & \frac{e^{\hat{b}}-e^{-\hat{b}}}{2} & \frac{e^{\hat{b}}-e^{-\hat{b}}}{2} & 1+\frac{e^{\hat{b}}+e^{-\hat{b}}}{2} \end{pmatrix} \quad (19)$$

where the differential operator $\hat{b} = \hbar\omega_{10}(R)d_{10}(R)\delta\cdot\partial/\partial P \equiv b\cdot\partial/\partial P$. Since $e^{\pm\hat{b}}$ are momentum translation operators, we see that the elements of this matrix operator produce small positive and negative momentum shifts scaled by the time step δ when they act on any function of the bath momenta. Thus, the action of this contribution to the nonadiabatic propagator on phase space functions produces a branching tree of classical trajectories, which leads to an exponential growth in the number of trajectories that must be followed. However, for small δ, Q_2 may be evaluated to linear order in δ to yield the simpler expression,

$$Q_2 \approx 1 + \frac{1}{2}\begin{pmatrix} 0 & 1 & 1 & 0 \\ 1 & 0 & 0 & 1 \\ 1 & 0 & 0 & 1 \\ 0 & 1 & 1 & 0 \end{pmatrix} b \cdot \frac{\partial}{\partial P} + \mathscr{O}(\delta^2) \equiv 1 + Ab \cdot \frac{\partial}{\partial P} + \mathscr{O}(\delta^2) \quad (20)$$

which is correct to the same order as the Trotter approximation used to evaluate the propagator. Using these expressions, we may write

$$e^{-\mathscr{J}\delta} = Q_1 + Q_1Ab \cdot \frac{\partial}{\partial P} + \mathscr{O}(\delta^2) \quad (21)$$

This expression is still not in a form that is suitable for computation since it involves the differential operator $\partial/\partial P$ which continuously produces small momentum changes in the bath as the system evolves nonadiabatically. However, as in earlier studies,[17,18] we may make the momentum-jump approximation that replaces the small continuous momentum changes with momentum jumps that accompany each quantum transition. To make the momentum-jump approximation, we work with each matrix element in eq 21, since each matrix element corresponds to a distinct possible quantum transition (or no transition). We may write the matrix elements of eq 21 in the form,

$$(e^{-\mathscr{J}\delta})_{ss'} = (Q_1)_{ss'} + (Q_1A)_{ss'}b \cdot \frac{\partial}{\partial P} + \mathscr{O}(\delta^2) = (Q_1)_{ss'}\left(1 + \frac{(Q_1A)_{ss'}b}{(Q_1)_{ss'}} \cdot \frac{\partial}{\partial P}\right) + \mathscr{O}(\delta^2) \equiv (Q_1)_{ss'}\left(1 + C_{ss'} \cdot \frac{\partial}{\partial P}\right) + \mathscr{O}(\delta^2) \quad (22)$$

where we have used the fact that $(Q_1A)_{ss'}b/(Q_1)_{ss'} = C_{ss'} + \mathscr{O}(\delta^2)$ with the matrix C given by

$$C = \begin{pmatrix} 0 & S_{01} & S_{01} & 2S_{01} \\ S_{10} & 0 & 0 & S_{01} \\ S_{10} & 0 & 0 & S_{01} \\ 2S_{10} & S_{10} & S_{10} & 0 \end{pmatrix} \quad (23)$$

where $S_{01} = \hbar\omega_{01}d_{01}/(2(P/M)\cdot d_{01})$ and $S_{10} = -S_{01}$. The terms involving S_{01} in this matrix correspond to transitions (00) → (01), (00) → (10), (01) → (11), or (10) → (11), that is, upward transitions to or from diagonal density element to the off-diagonal density elements (01) or (10). Also, the terms involving S_{10} correspond to transitions (10) → (00), (01) → (00), (11) → (10), or (11) → (01); that is, a similar set of downward transitions. The terms involving $2S_{01}$ and $2S_{10}$ correspond to transitions (00) ⇌ (11); that is, transitions between the ground and the excited states.

The momentum jump approximation to this propagator entails the approximation of the sum $(1 + C_{ss'}\cdot\partial/\partial P)$ by an exponential to give

$$(e^{-\mathscr{L}\delta})_{ss'} \approx (Q_1)_{ss'}\, e^{C_{ss'}\cdot\partial/\partial P} + \mathscr{O}(\delta^2) \equiv \mathscr{M}_{ss'}(\delta) + \mathscr{O}(\delta^2) \quad (24)$$

The last line defines the matrix $\mathscr{M}$ whose explicit form is

$$\mathscr{M}(\delta) = \begin{pmatrix} \cos^2(a) & -\cos(a)\sin(a)\hat{j}_{01} & -\cos(a)\sin(a)\hat{j}_{01} & \sin^2(a)\hat{j}_{0\to1} \\ \sin(a)\cos(a)\hat{j}_{10} & \cos^2(a) & -\sin^2(a) & -\sin(a)\cos(a)\hat{j}_{01} \\ \sin(a)\cos(a)\hat{j}_{10} & -\sin^2(a) & \cos^2(a) & -\sin(a)\cos(a)\hat{j}_{01} \\ \sin^2(a)\hat{j}_{1\to0} & \sin(a)\cos(a)\hat{j}_{10} & \sin(a)\cos(a)\hat{j}_{10} & \cos^2(a) \end{pmatrix} \quad (25)$$

In this equation, $\hat{j}_{\alpha\beta}$ is defined as $\hat{j}_{\alpha\beta} = \exp(S_{\alpha\beta}\cdot\nabla_P)$. Since $S_{\alpha\beta} = \hbar\omega_{\alpha\beta}M\hat{d}_{\alpha\beta}/(2P\cdot\hat{d}_{\alpha\beta})$ is a function of P, the action of the operator in this form on any function of the momenta P cannot be represented as a simple momentum translation. Here, $\hat{d}_{\alpha\beta}$ is the unit vector along $d_{\alpha\beta}$. However, it is easy to demonstrate that it is a momentum translation operator in $(\hat{d}_{\alpha\beta}\cdot P)^2$ in the following way.[17] We may write $S_{\alpha\beta}\cdot\partial/\partial P = \hbar\omega_{\alpha\beta}M\cdot\partial/\partial(\hat{d}_{\alpha\beta}\cdot P)^2$. In any function $f(P)$, P may be decomposed into its components along and normal to $\hat{d}_{\alpha\beta}$ as $P = (1 - \hat{d}_{\alpha\beta}\hat{d}_{\alpha\beta})\cdot P + \hat{d}_{\alpha\beta}(\hat{d}_{\alpha\beta}\cdot P) \equiv P_\perp + \hat{d}_{\alpha\beta}(\hat{d}_{\alpha\beta}\cdot P) = P_\perp + \hat{d}_{\alpha\beta}\,\mathrm{sgn}(\hat{d}_{\alpha\beta}\cdot\mathbf{P})\sqrt{(\hat{d}_{\alpha\beta}\cdot\mathbf{P})^2}$. Using these results, we have

$$\begin{aligned} \hat{j}_{\alpha\beta}f(P) &= e^{S_{\alpha\beta}\cdot\partial/\partial P}f(P) \\ &= e^{\hbar\omega_{\alpha\beta}M\partial/\partial(\hat{d}_{\alpha\beta}\cdot P)2)}\, f(P_\perp + \hat{d}_{\alpha\beta}\,\mathrm{sgn}(\hat{\mathbf{d}}_{\alpha\beta}\cdot\mathbf{P})\sqrt{(\hat{\mathbf{d}}_{\alpha\beta}\cdot\mathbf{P})^2}) \\ &= f(P + \Delta P_{\alpha\beta}) \end{aligned} \quad (26)$$

In writing the last line of this equation, we used the fact that $\exp(\hbar\omega_{\alpha\beta}M\partial/\partial(\hat{d}_{\alpha\beta}\cdot P)^2))$ is a translation operator on $(\hat{d}_{\alpha\beta}\cdot P)^2$, and we defined $\Delta P_{\alpha\beta} = \hat{d}_{\alpha\beta}\,(\mathrm{sgn}(\hat{d}_{\alpha\beta}\cdot P)\sqrt{(\hat{d}_{\alpha\beta}\cdot P)^2 + \hbar\omega_{\alpha\beta}M} - (\hat{d}_{\alpha\beta}\cdot P))$.

Similarly, the double jump operators that produce transitions between the ground and excited states are given by $\hat{j}_{\alpha\to\beta} = \exp(2S_{\alpha\beta}\cdot\nabla_P)$, and their action on $f(P)$ is

$$\hat{j}_{\alpha\to\beta}f(P) = e^{2\hbar\omega_{\alpha\beta}M\partial/\partial(\hat{d}_{\alpha\beta}\cdot P)2)}f(P) = f(P + \Delta P_{\alpha\to\beta}) \quad (27)$$

with $\Delta P_{\alpha\to\beta} = \hat{d}_{\alpha\beta} \times (\mathrm{sgn}(\hat{d}_{\alpha\beta}\cdot P)\sqrt{(\hat{d}_{\alpha\beta}\cdot P)^2 + 2\hbar\omega_{\alpha\beta}M} - (\hat{d}_{\alpha\beta}\cdot P))$.

We may verify that the energy of the system is conserved under quantum-classical dynamics by showing that the matrix elements of the total Hamiltonian in the adiabatic basis, $H_s(R, P)$, are invariant under the time propagation,

$$\sum_{s_1} e^{i\mathscr{L}^0_{s_0}\delta/2}\mathscr{M}_{s_0s_1}\, e^{i\mathscr{L}^0_{s_1}\delta/2}H_{s_1} = H_{s_0} \quad (28)$$

First, note that the vector H_{s_1} whose elements are ($H_0(R, P) = P^2/2M + E_0(R)$, $H_1(R, P) = H_2(R, P) = 0$, and $H_3(R, P) = P^2/2M + E_1(R)$), is invariant under adiabatic dynamics $e^{i\mathscr{L}^0_{s_1}\delta/2}H_{s_1}(R, P) = H_{s_1}(R, P)$. Adiabatic dynamics is the classical evolution of the bath in the Hellmann−Feynman field of an adiabatic state and thus conserves energy. So we need only show that $\sum_{s_1}\mathscr{M}_{s_0s_1}H_{s_1}(R, P) = H_{s_0}(R, P)$, which results from the direct multiplication of the matrix $\mathscr{M}$ with the vector H and use of the relations

$$\begin{aligned} \hat{j}_{1\to0}H_0 &= \hat{j}_{1\to0}(P^2/2M + E_0(R)) = \\ &\quad ((P + \Delta P_{0\to1})^2/2M + E_0(R)) = H_3 \\ \hat{j}_{0\to1}H_3 &= \hat{j}_{0\to1}(P^2/2M + E_1(R)) = \\ &\quad ((P + \Delta P_{1\to0})^2/2M + E_1(R)) = H_0 \end{aligned} \quad (29)$$

and

$$\begin{aligned} \hat{j}_{10}H_0 &= P^2/2M + (E_0(R) + E_1(R))/2 \\ \hat{j}_{01}H_3 &= P^2/2M + (E_0(R) + E_1(R))/2 \end{aligned} \quad (30)$$

In eq 29, the third equality follows by direct substitution of the explicit expression for $\Delta P_{0\to1}$.

Resulting Form of Surface-Hopping Representation. Inserting the previous results in the original Trotter expansion (eq 13), we have

$$\begin{aligned} (e^{i\mathscr{L}(t_j - t_{j-1})})_{s_{j-1}s_j} &\approx e^{i\mathscr{L}^0_{s_{j-1}}\delta/2}\mathscr{M}_{s_{j-1}s_j}(\delta)\, e^{i\mathscr{L}^0_{s_j}\delta/2} = \\ &\mathscr{W}_{s_{j-1}}(t_{j-1}, t_j - \delta/2)\, e^{iL_{s_{j-1}}\delta/2}\mathscr{M}_{s_{j-1}s_j}(\delta)\,\mathscr{W}'_{s_j}(t_j - \delta/2, t_j)\, e^{iL_{s_j}\delta/2} \end{aligned} \quad (31)$$

Thus, we see that the short-time propagator represents, reading from left to right, (1) classical propagation on the s_{j-1} surface through a time interval $\delta/2$. This evolution will involve a phase factor if the s_{j-1} index corresponds to a pair of different adiabatic states; (2) a transition $s_{j-1} \to s_j$ determined by the elements of $\mathscr{M}$. Momentum changes in the bath are accounted for by the momentum jump operators in this matrix; (3) classical propagation on the s_j surface for a time interval $\delta/2$. The full evolution is determined from the concatenation of evolutions over these short time segments. These three steps constitute the surface-hopping representation of the quantum-classical propagator. In the next section, we describe how this propagator can be simulated on the basis of the above formulation of the problem.

3. Simulation Algorithm

The method used to simulate the dynamics and compute the expectation value of an observable $\hat{B}_W(R, P, t)$ in eq 4 is based on the development of the quantum-classical propagator as a product of short time segments leading to eq 12. Using eq 31, we may write the expression for $\overline{B(t)}$ more explicitly as

$$\overline{B(t)} = \sum_{s_0}\int \mathrm{d}R\,\mathrm{d}P\, B_W^{s_0}(R,P,t)\rho_W^{s_0'}(R,P) = \sum_{s_0}\int \mathrm{d}R\,\mathrm{d}P\,\rho_W^{s_0'}(R,P)\times \sum_{s_1,\cdots,s_N}\left[\prod_{j=1}^{N}\mathscr{W}'_{s_{j-1}}(t_{j-1},t_j-\delta/2)\times \mathrm{e}^{iL_{s_{j-1}}\delta/2}\mathscr{M}_{s_{j-1}s_j}(\delta)\mathrm{W}_{s_j}(t_j-\delta/2,t_j)\,\mathrm{e}^{iL_{s_j}\delta/2}\right]B_W^{s_N}(R,P) \quad (32)$$

where $s_0' = (\alpha_0', \alpha_0)$ is obtained from $s_0 = (\alpha_0, \alpha_0')$ by the interchange $\alpha_0 \rightleftharpoons \alpha_0'$. The summations in the indices and the phase space integral can be performed through Monte Carlo sampling, but there remains the question of how to evaluate the sequences of propagators that appear in the integrand at successive time slices where the short time propagator itself is complicated. Such calculations are easy to compute only proceeding from left to right as we now discuss.

Consider a sequence of evolution operators acting on a function $f(x)$, for example, $O_1O_2O_3f(x)$ where

$$O_1f(x) = \varphi_1(x)f(o_1(x)),\quad O_2f(x) = \varphi_2(x)f(o_2(x)),\quad O_3f(x) = \varphi_3(x)f(o_3(x)) \quad (33)$$

The $\varphi_1(x)$, $\varphi_2(x)$, and $\varphi_3(x)$ denote multiplicative functions and $o_1(x)$, $o_2(x)$, and $o_3(x)$ denote functions representing the effect of the operator on the argument of f. Mathematically,

$$O_1O_2O_3f(x) = \varphi_1(x)\varphi_2(o_1(x))\varphi_3(o_2(o_1(x)))f(o_3(o_2(o_1(x)))) \quad (34)$$

Such sequences of operations are easy to compute recursively going from left to right (the opposite order from right to left is not recursive and is difficult to perform), since

$$O_1O_2O_3(f(x)) = O_1[O_2O_3f(x)] = \varphi_1(x)[O_1O_2f(x_1)],\ x_1 = o_1(x)$$

$$O_2O_3(f(x_1)) = O_2[O_3f(x_1)] = \varphi_2(x_1)[O_3f(x_2)],\ x_2 = o_2(x_1)$$

$$O_3f(x_2) = \varphi(x_2)f(x_3), x_3 = o_3(x_2)$$

This is also true if O_1, O_2, and O_3 are matrices of evolution operators, since their product can be reduced to sums of products of the above type. Hence, if we combine Monte Carlo sampling of indices and phase space points (where the role of x above is played by the initial point in phase space of a trajectory) with recursive propagation, we observe that the full quantum-classical propagator can be calculated in terms of surface-hopping trajectories. The simulation algorithm consists then of three steps based on the structure of eq 32. For simplicity, we divide the total time of the simulation into t/δ short time segments. Using the form of the short time propagator in eq 31, we can rearrange eq 32 into the Monte Carlo form

$$\overline{B(t)} = \frac{\mathscr{N}^2}{M}\sum_{\kappa=1}^{M}\frac{\rho_W^{s_0'^{\kappa}(R^\kappa,P^\kappa)}}{|\rho_W^{s_0'^{\kappa}(R^\kappa,P^\kappa)}|}\times \left[\prod_{j=1}^{t/\delta}\left(\mathscr{W}'_{s_{j-1}^\kappa}(t_{j-1},t_j-\delta/2)\,\mathrm{e}^{iLs_{j-1}^\kappa\delta/2}\frac{\sum_{s_j^\kappa}|(Q_1)_{s_{j-1}^\kappa s_j^\kappa}(\delta)|}{|(Q_1)_{s_{j-1}^\kappa s_j^\kappa}(\delta)|}\times \mathscr{M}_{s_{j-1}^\kappa s_j^\kappa}(\delta)\mathscr{W}'_{s_j^\kappa}(t_j-\delta/2,t_j)\,\mathrm{e}^{iL_{s_j^\kappa}\delta/2}\right)_{s_{j-1}^\kappa s_j^\kappa}\right]B_W^{s_N^\kappa}(R^\kappa,P^\kappa) \quad (35)$$

where the index κ refers to the Monte Carlo sampling of the elementary event $(R^\kappa, P^\kappa, s_0'^\kappa, s_1^\kappa, \cdots, s_N^\kappa)$ and the elements of the $\mathscr{M}$ matrix are defined in eq 25. The $\mathscr{N}^2$ factor comes from the uniform sampling for the sum on the initial states s_0. Phase space is importance sampled according to $|\rho_W^{s_0'}(R,P)|$, which leaves in the sum the phase factor, $\sigma = \rho_W^{s_0'}(R,P)/|\rho_W^{s_0'}(R,P)|$. To continue the procedure, we need to mix Monte Carlo sampling and propagation. The first step ($j = 1$) includes (a) classical propagation of phase space point (R, P) to $\mathrm{e}^{iL_{s_0}\delta/2}(R,P) = (R',P')$ and updating of the phase factor W_{s_0} and all of the matrix elements and operators, including the observable, at the value of this evolved phase point; (b) choice of the value of the index s_1 in the matrix $\mathscr{M}_{s_0s_1}(\delta)$ by sampling with probability $|(Q_1)_{s_0^\kappa s_1^\kappa}(\delta)|/\sum_{s_1^\kappa}|(Q_1)_{s_0^\kappa s_1^\kappa}(\delta)|$. This introduces the factor $\sum_{s_1^\kappa=0}^{3}|(Q_1)_{s_0^\kappa s_1^\kappa}(\delta)|/|(Q_1)_{s_0^\kappa s_1^\kappa}(\delta)|$. (c) Once the index s_1 is selected, the momentum jump (if any) specified by $\mathscr{M}_{s_0s_1}(\delta)$ is applied to all functions and operators to its right so that the new bath phase space point is $(R', \bar{P}')$, where the overline denotes the momentum after the momentum-jump operation. (d) The phase factor $\mathscr{W}'_{s_1}$ is computed and the evolution operator $\mathrm{e}^{iL_{s_1}\delta/2}$ is used to propagate the bath phase space coordinates $(R', \bar{P}')$ to time t_1:$\mathrm{e}^{iL_{s_1}\delta/2}(R', \bar{P}') = (R'', P'')$. To continue the propagation, the procedure is repeated starting from the index $j = 2$ in the product in eq 35 with the updated value of the bath phase space point.

This algorithm has features in common with the sequential short-time propagation (SSTP) algorithm introduced earlier.[34,35] It differs in the following respects: the nonadiabatic propagator $\exp(-\mathscr{J}\delta)$ described by the matrix $\mathscr{M}$ in eq 25 was derived from a Trotter decomposition. In the SSTP algorithm, this propagator was simply approximated by $\exp(-\mathscr{J}\delta) \approx 1 - \mathscr{J}\delta$. The function $(P/M)\cdot d_s$, which determines the probabilities with which nonadiabatic transitions occur, appears as the argument of trigonometric functions in $\mathscr{M}$, while this quantity appears in linear functions in the SSTP algorithm. More generally, the unitary exponential character of the evolution operator in the Trotter decomposition leads to an algorithm with a much firmer basis.

In order to complete the specification of the simulation scheme, we now describe another essential component of the algorithm. Estimates of averages computed using the above steps are dominated by large fluctuations which come from unusually large values of the summand of eq 35. These fluctuations are due to the factors in the integrand containing the matrix Q_1. These large factors exacerbate the sign problem that comes from the phase factors in the evolution and make it difficult to obtain accurate MC estimates of the observable. These fluctuations can be eliminated in part by using a filter similar to that described in ref 37 that eliminates improperly large biasing fluctuations which should not contribute to the averaged quantity. In its simplest form, the filter is implemented by putting an upper bound on the magnitude of the factor in the square

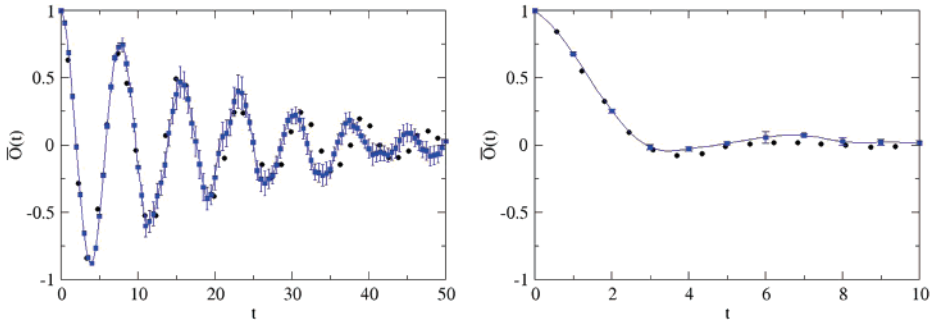

Figure 1. Exact quantum results from ref 40 (●), TBQC algorithm (□) (a, left) $\beta = 12.5$, $\xi = 0.09$, and $\Omega = 0.4$; (b, right) $\beta = 0.25$, $\xi = 0.09$, and $\Omega = 0.4$.

brackets appearing in the summand in eq 35. When, at stage j in the calculation of the product in the summand, the running summand exceeds the bound, the factor in the updating of the running product is put to unity and the index s_j is put to s_{j-1}.

The value of the bound depends on the nonadiabaticity of the system and the duration of the simulation. In addition, in order to minimize the size of the ensemble required to estimate expectation values of observables, it is necessary to choose the largest possible size of the time interval δ, consistent with a negligible error in the Trotter approximation. The filter must be used for medium and long time simulations.

The time step δ and the filter parameters can be determined by first simulating the dynamics for various value of δ for a short time without the filter and monitoring the convergence of the results as δ is decreased. The largest value of δ needed to obtain converged results may be used in subsequent simulations. Also, although the filter is not required for short times, a filter may be employed, and the smallest value of the bound which reproduces the previously obtained converged results may be determined. If needed, for longer-time simulations, one may increase the bound further until convergence is obtained.

4. Spin-Boson Model

The spin-boson model[38,39] is one of the most popular testing grounds for simulation schemes for many-body quantum dynamics since numerically exact full quantum results are available for this model.[8,9,40−43] As such, it provides an important test of the accuracy of our surface-hopping method for simulating quantum-classical dynamics. In addition, it captures the essential elements of a variety of quantum rate phenomena in open quantum systems and has been used to model many physical and chemical systems.[39]

The spin-boson model describes a two-level system with states $|\uparrow\rangle$ and $|\downarrow\rangle$ bilinearly coupled to a bath of N harmonic oscillators. For this model, quantum-classical Liouville dynamics in eq 6 (or the corresponding equation of motion for the density matrix) is exact[24] so a full test of the simulation scheme can be made without having to consider the validity of the assumptions that underlie the application of this method to any particular real system. The partially Wigner transformed spin-boson Hamiltonian is

$$\hat{H}_W = -\hbar\Omega\hat{\sigma}_x + \sum_{j=1}^{N}\left(\frac{P_j^2}{2M_j} + \frac{1}{2}M_j\omega_j^2R_j^2 - c_jR_j\hat{\sigma}_z\right) \quad (36)$$

where the bath oscillators have masses M_j and frequencies ω_j and $\hat{\sigma}_x$ and $\hat{\sigma}_z$ are Pauli spin matrices. We simulate a spin-boson system with an Ohmic spectral density characterized by the Kondo parameter ξ and frequency ω_c. The values of the parameters were taken from Makri and Thompson[8] and are given by $c_j = (\xi\hbar\omega_0M_j)^{1/2}\omega_j$, $\omega_j = -\omega_c \ln(1 - j\omega_0/\omega_c)$ where $\omega_0 = \omega_c(1 - \exp(-\omega_{max}/\omega_c))/N$ and $j = 1, ..., N$. The parameter $\omega_{max} = 3\omega_c$ is a cutoff frequency. Further details of the model, along with the forms of the adiabatic states and non-adiabatic coupling matrix elements, can be found in ref 24. Dimensionless variables are used in reporting the numerical results, with the energy ($\hbar\Omega$) and inverse temperatures $\beta = 1/k_BT$ given in units of $\hbar\omega_c$.

We consider the computation of the average value of the population difference for which the observable in eq 4 is $\hat{B}_W(R, P) = \hat{\sigma}_z$,

$$\overline{\sigma_z(t)} = \mathrm{Tr}' \int \mathrm{d}R\, \mathrm{d}P\, \hat{\sigma}_z(t)\hat{\rho}(R, P) \quad (37)$$

In order to compare with previously obtained exact results, the initial value of the density matrix is taken to be the product of subsystem and bath density matrices,

$$\hat{\rho}_W(R, P) = |\uparrow\rangle\langle\uparrow|\rho_W^{(b)}(R, P) \quad (38)$$

The subsystem density matrix is $|\uparrow\rangle\langle\uparrow|$ corresponding to the subsystem in state $|\uparrow\rangle$. Two different forms of the bath density have been employed in the literature to obtain the exact quantum results with which we compare our simulation results. The bath density matrix is either that for the quantum bath in internal thermal equilibrium,

$$\rho_{We}^{(b)}(R', P') = \prod_{j=1}^{N}\frac{\tanh(\beta\omega_j/2)}{\pi}\exp\left[-\frac{2\tanh(\beta\omega_j/2)}{\omega_j}\left(\frac{P_j'^2}{2} + \frac{\omega_j^2R_j'^2}{2}\right)\right] \quad (39)$$

or the canonical density, $\rho_{Wn}^{(b)}$. The latter form may be obtained from eq 39 by the replacement $R_j' \rightarrow R_j' - c_i/\omega_i^2$. Equation 39 is expressed in the dimensionless variables $R_j' = (M_j\omega_c/\hbar)^{1/2}R_j$, $P_j' = (\hbar M_j\omega_c)^{-1/2}P_j$.

Results

To investigate the validity and scope of the TBQC algorithm, the time dependence of the average population difference for a wide variety of system parameters (non-adiabatic coupling strength, temperature, and quantum subsystem energies) was simulated and compared with exact results. In all cases, error bars were estimated. In the figures, the initial density matrix corresponds to $\rho_{Wn}^{(b)}$ with the exception of Figure 2 where it is $\rho_{We}^{(b)}$. The number of time slices in each figure equals the number of TBQC data points denoted by the □ symbol and the Ohmic bath consisted of 200 oscillators. The MD integration time step was 0.1 (in dimensionless units). In the figures involving relatively long simulation times (Figures 1a and 3a), 10^5 trajectories were used to obtain converged results. The decay

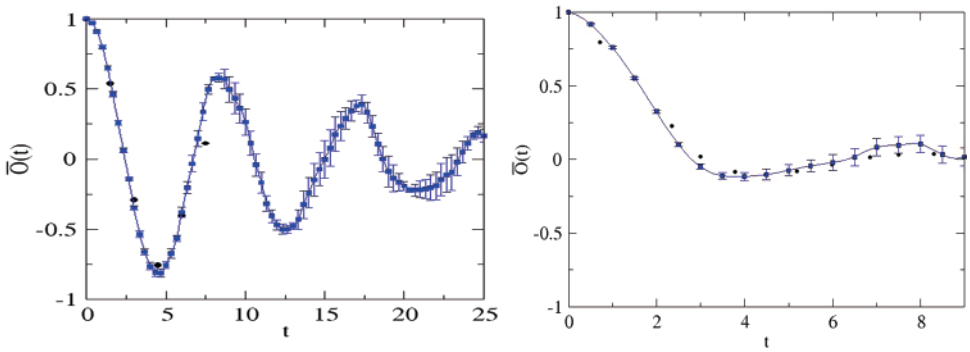

Figure 2. Exact quantum results from ref 8 (●), TBQC algorithm (□) (a, left) $\beta = 3$, $\xi = 0.1$, and $\Omega = 1/3$; (b, right) $\beta = 3$, $\xi = 0.5$, and $\Omega = 1/3$.

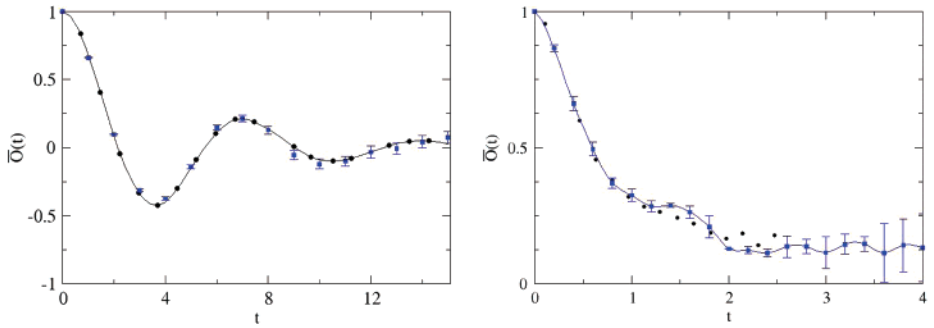

Figure 3. TBQC algorithm (□), (a, left) exact quantum results from refs 41 and 42 (●), $\beta = 1$, $\xi = 0.13$, and $\Omega = 0.4$; (b, right) exact quantum results from ref 43 (●), $\beta = 0.25$, $\xi = 2$, and $\Omega = 1.2$.

rates in these cases can be estimated with only 10^4 trajectories. All of the other simulations used 2×10^4 trajectories. In all cases, two nonadiabatic transitions were required to obtain agreement with the exact results. Figure 1a shows the slow decay of the oscillations in the population difference for weak subsystem-bath coupling $\xi = 0.09$ and a low temperature $\beta = 12.5$. The oscillations are highly damped in Figure 1b for a high temperature, $\beta = 0.25$. In both cases, the simulations agree well with the exact quantum results, although in Figure 1a the phase coherence is lost for long times as result of errors that arise because of our sampling scheme. One may compare our results with those of other simulation methods for these parameter choices (cf. Figure 5 of ref 44 and Figure 2 of ref 14). Comparable agreement is found, although the loss of phase coherence sets in at different times depending on the precision of the various simulation methods for the parameter set in Figure 1a.

Figure 2 presents a comparison of results for low ($\xi = 0.1$) and high ($\xi = 0.5$) friction for $\beta = 3$ and $\Omega = 1/3$. Our results are in close agreement with the exact quantum results. For comparison, see Figure 4 of ref 14. Finally, we consider systems with a larger energy gaps, $\Omega = 0.4$ and $\Omega = 1.2$, in Figure 3. Once again, our simulations are able to reproduce the exact quantum results for this model. Comparison results may be found in Figures 1 and 2 of ref 42, Figures 2b and 3a of ref 14, and Figures 7a and 6b of ref 44.

These simulation results confirm that the TBQC algorithm is able to accurately reproduce the exact quantum results for the spin-boson model over a wide range of coupling strengths and temperatures. The method is capable of following the dynamics for times which are three to four times longer than is possible using the SSTP algorithm. The ability of the Trotter algorithm to simulate the dynamics for longer times than the SSTP algorithm is especially evident for some parameter regimes, especially for high values of the friction. For example, the SSTP algorithm tends to fail for $\beta = 3$ and $\Omega = 2/3$ for values of the friction $\xi > 0.1$. The Trotter-based quantum-classical algorithm described here will allow one to extend the class of problems that can be studied using quantum-classical Liouville dynamics.

5. Conclusion

The Trotter-based algorithm for simulating quantum-classical Liouville dynamics is able to reproduce the numerically exact full quantum results for the spin-boson model for longer times and for a wider range of coupling strengths than the sequential short time propagation algorithm. The results are of comparable accuracy to those of many schemes for simulating quantum dynamics for this system.[14,42,44]

A few aspects of our results merit further comment. As discussed earlier, quantum-classical Liouville dynamics is exact for the spin-boson model. Expectation values and correlation functions are also exact provided the initial or equilibrium states are sampled for the full quantum distributions. The simulation algorithm employs the momentum-jump approximation in the computation of the nonadiabatic propagator. The fact that our simulation results are in accord with the exact quantum results confirms the validity of this approximation for the spin-boson model. The discrepancies at long times can be attributed to the difficulties associated with Monte Carlo sampling discussed in the text.

Although calculations cannot be extended to arbitrarily long times due to these sampling problems, the combination of the Trotter scheme for the nonadiabtic propagator and the implementation of filtering has allowed us to greatly extend the accessible time and the range of coupling strengths and temperatures that can be considered. Furthermore, the structure of the nonadiabtic propagator leads to a surface-hopping dynamics that exactly conserves energy when nonadiabatic transitions take place, regardless of whether these transitions are to pairs of different adiabatic states or pairs of the identical adiabatic states.

While this study has focused on the spin-boson model, the algorithm presented here can be applied to any quantum subsystem described by a small manifold of quantum states coupled in any way to a bath described by any potential energy function. For instance, quantum-classical Liouville dynamics has been used to study condensed phase proton-transfer processes,[37,45,46] and the TBQC algorithm can be used to study complex systems of this type. Quantum bath nuclear dispersion effects may also be taken into account by suitable sampling of initial or equilibrium quantum distributions. In this case, only the dynamics is approximated by the quantum-classical Liouville equation. This feature, in combination with the simulation algorithm discussed here, will greatly extend the domain of applicability and utility of quantum-classical Liouville dynamics and its simulation in terms of surface-hopping trajectories.

Acknowledgment. D.M. is grateful to Werner Blau and Charles Patterson for the opportunity and encouragement to complete this work in Dublin. He also acknowledges the support of the Science Foundation Ireland and the Irish High Education Authority through the PRTLI (IATAC) programme, an EU-ESF COST visiting scientist grant via the MOLSIMU programme (Action P13), and a visiting scientist grant from CNISM (Italian National inter-university consortium for the physics of matter). The research of R.K. was supported in part by a grant from the Natural Sciences and Engineering Research Council of Canada.

Appendix

A: Diagonalization of J_1 and J_2. For a two state sub-system, one can show that J_1

$$J_1 = -\begin{pmatrix} 0 & 1 & 1 & 0 \\ -1 & 0 & 0 & 1 \\ -1 & 0 & 0 & 1 \\ 0 & -1 & -1 & 0 \end{pmatrix} \frac{P}{M}\cdot d(R) \tag{40}$$

can be written in the form $J_1 = V^{-1}D_1V$ with

$$V = \begin{pmatrix} 1 & 0 & -1 & -1 \\ 0 & -1 & -\imath & \imath \\ 0 & 1 & -\imath & \imath \\ 1 & 0 & 1 & 1 \end{pmatrix}, V^{-1} = \begin{pmatrix} \frac{1}{2} & 0 & 0 & \frac{1}{2} \\ 0 & \frac{-1}{2} & \frac{1}{2} & 0 \\ \frac{-1}{4} & \frac{\imath}{4} & \frac{\imath}{4} & \frac{1}{4} \\ \frac{-1}{4} & \frac{-\imath}{4} & \frac{-\imath}{4} & \frac{1}{4} \end{pmatrix} \tag{41}$$

where V is the matrix of eigenvectors and V^{-1} is its inverse. The diagonal matrix of eigenvalues is D_1 whose diagonal elements are $\{0, 0, -2\imath\, P/M\cdot d, 2\imath\, P/M\cdot d\}$. Similarly,

$$J_2 = -\begin{pmatrix} 0 & 1 & 1 & 0 \\ 1 & 0 & 0 & 1 \\ 1 & 0 & 0 & 1 \\ 0 & 1 & 1 & 0 \end{pmatrix} \frac{\hbar\omega_{10}(R)d(R)\cdot\left(\frac{\partial}{\partial P}\right)}{2} \tag{42}$$

with $\hbar\omega_{10}(R) = E_1(R) - E_0(R)$ may be written as $J_2 = K^{-1}D_2K$ with

$$K = \begin{pmatrix} 1 & -1 & 0 & 1 \\ 1 & 0 & -1 & -1 \\ 1 & 0 & 1 & -1 \\ 1 & 1 & 0 & 1 \end{pmatrix}, K^{-1} = \begin{pmatrix} \frac{1}{4} & \frac{1}{4} & \frac{1}{4} & \frac{1}{4} \\ \frac{-1}{2} & 0 & 0 & \frac{1}{2} \\ 0 & \frac{-1}{2} & \frac{1}{2} & 0 \\ \frac{1}{4} & \frac{-1}{4} & \frac{-1}{4} & \frac{1}{4} \end{pmatrix} \tag{43}$$

where K and K^{-1} are the matrix of eigenvectors and its inverse, respectively. The diagonal matrix of eigenvalues D_2 has diagonal elements$\{-\hbar\omega_{10}(R)d(R)\cdot\partial/\partial P, 0, 0, \hbar\omega_{10}(R)d(R)\cdot\partial/\partial P\}$.

B: Multi-State Subsystem. The quantum-classical dynamics of an $\mathcal{N}$-state quantum system can be computed using eqs 12 and 13 where the matrix propagators have dimension $\mathcal{N}^2 \times \mathcal{N}^2$. In this Appendix, we show how the nonadiabatic propagator in this formula can be computed without resorting to numerical diagonalization.

The nonadiabatic transition operator $\mathcal{J}$ is proportional to the nonadiabatic coupling matrix elements $d_{\alpha\beta}$ which satisfy the symmetry relations $d_{\alpha\beta} = -d^*_{\beta\alpha}$. Thus, for an $\mathcal{N}$-level system, there are $\mathcal{J} = 1/2\,\mathcal{N}(\mathcal{N}-1)$ distinct nonadiabatic coupling matrix elements, and the nonadiabatic transition operator $\mathcal{J}$ can be written as a sum on $\mathcal{J}$ terms, each of which is proportional to a distinct $d_{\alpha\beta}$ with $\alpha > \beta$,

$$\mathcal{J} = \sum_{l=1}^{\mathcal{J}} \mathcal{J}^{(l)} \tag{44}$$

Using a Trotter factorization, the short time nonadiabatic propagator can be written as

$$e^{-\mathcal{J}\delta} = e^{-\sum_{l=1}^{\mathcal{J}}\mathcal{J}^{(l)}\delta} \approx \prod_{l=1}^{\mathcal{J}} e^{-\mathcal{J}^{(l)}\delta} + \mathcal{O}(\delta^2) \tag{45}$$

As for the two-level system, each of the nonadiabatic transition operators can be written as the sum of two terms, one of which is proportional to P and the other to $\partial/\partial P$, leading to the additional Trotter factorization,

$$e^{-\mathcal{J}^{(l)}\delta} \approx e^{-J_1^{(l)}\delta} e^{-J_2^{(l)}\delta} + \mathcal{O}(\delta^2) \tag{46}$$

The problem of the calculation of the $\mathcal{N}$-state nonadiabatic propagator is now reduced to the calculation of the propagators corresponding to transitions between pairs of states in the $\mathcal{N}$-level system.

For each pair of indices representing a pair of adiabatic states (μ, γ), $\mu > \gamma$, we have

$$J^{(l)}_{1\alpha\alpha',\beta\beta'} = -d_{\mu\gamma}\cdot\frac{P}{M}((\delta_{\mu\alpha}\delta_{\gamma\beta} - \delta_{\gamma\alpha}\delta_{\mu\beta})\delta_{\alpha'\beta'} + (\delta_{\mu\alpha'}\delta_{\gamma\beta'} - \delta_{\gamma\alpha'}\delta_{\mu\beta'})\delta_{\alpha\beta}) \tag{47}$$

and

$$J^{(l)}_{2\alpha\alpha',\beta\beta'} = -\frac{1}{2}\hbar\omega_{\mu\gamma}d_{\mu\gamma}\cdot\frac{\partial}{\partial P}((\delta_{\mu\alpha}\delta_{\gamma\beta} + \delta_{\gamma\alpha}\delta_{\mu\beta})\delta_{\alpha'\beta'} + (\delta_{\mu\alpha'}\delta_{\gamma\beta'} + \delta_{\gamma\alpha'}\delta_{\mu\beta'})\delta_{\alpha\beta}) \tag{48}$$

It follows directly from eqs 47 and 48 that the vector space corresponding to this representation consists of a four-dimensional invariant space spanned by the set of states $\{(\gamma\gamma), (\gamma\mu), (\mu\gamma), (\mu\mu)\}$, and $2(\mathcal{N}-2)$ two-dimensional vector spaces spanned by $\{(\gamma, \alpha'), (\mu\alpha')\}$ for $\alpha' \neq \mu, \gamma$, and

$\{(\alpha\gamma), (\alpha\mu)\}$ $\alpha \neq \mu, \gamma$. The complement of these vector spaces is an $(\mathcal{N}-2)^2$-dimensional null space.

With a suitable permutation of the pairs of states, the $\mathcal{J}^{(l)}$ matrices may be written in block diagonal forms consisting of a single 4×4 block, $2(\mathcal{N}-2)$ 2×2 blocks and a $(\mathcal{N}-2)^2 \times (N-2)^2$ block corresponding to a null space. The 4×4 blocks have structures identical to those for the two level system discussed in the text. The 2×2 blocks have a simple structure. For instance, letting $\mathcal{J}^{(l)}_{2\times2}$ be the 2×2 matrix spanned by the states $\{(\gamma\alpha'), (\mu\alpha')\}$ with $\alpha' \neq \gamma, \mu$, these blocks corresponding to the $\mathcal{J}^{(l)}_1$ and $\mathcal{J}^{(l)}_2$ matrices have the explicit forms

$$\mathcal{J}^{(l)}_{1,2\times2} = \begin{pmatrix} 0 & -1 \\ 1 & 0 \end{pmatrix} \frac{P}{M} \cdot d_{\mu\gamma}(R) \tag{49}$$

which has eigenvalues $\pm\imath\, P/M \cdot d_{\mu\gamma}(R)$, and

$$\mathcal{J}^{(l)}_{2,2\times2} = -\begin{pmatrix} 0 & 1 \\ 1 & 0 \end{pmatrix} \frac{1}{2}\, \omega_{\mu\gamma}(R) d_{\mu\gamma}(R) \cdot \frac{\partial}{\partial P} \tag{50}$$

with eigenvalues $\pm 1/2\, \hbar\omega_{\mu\gamma} d_{\mu\gamma}(R) \cdot \partial/\partial P = \pm b_{\mu\gamma}(R) \cdot \partial/\partial P$. The corresponding propagators have the form

$$\mathrm{e}^{-J^{(l)}_{1,2\times2}\delta} = \begin{pmatrix} \cos(a_{\mu\gamma}) & \sin(a_{\mu\gamma}) \\ -\sin(a_{\mu\gamma}) & \cos(a_{\mu\gamma}) \end{pmatrix} \tag{51}$$

with $a_{\mu\gamma} = \delta\, P/M \cdot d_{\mu\phi}(R)$, and

$$\mathrm{e}^{-J^{(l)}_{2,2\times2}\delta} = \frac{1}{2}\begin{pmatrix} e^{\hat{b}_{\mu\gamma}} + e^{-\hat{b}_{\mu\gamma}} & e^{\hat{b}_{\mu\gamma}} - e^{-\hat{b}_{\mu\gamma}} \\ e^{\hat{b}_{\mu\gamma}} - e^{-\hat{b}_{\mu\gamma}} & e^{\hat{b}_{\mu\gamma}} + e^{-\hat{b}_{\mu\gamma}} \end{pmatrix} \tag{52}$$

where $\hat{b}_{\mu\gamma} = \delta\, 1/2\, \hbar\omega_{\mu\gamma} d_{\mu\gamma}(R) \cdot \nabla_P$. As for the two-level system, we may write eq 52 as

$$\mathrm{e}^{-J^{(l)}_{2,2\times2}\delta} \approx 1 + \begin{pmatrix} 0 & 1 \\ 1 & 0 \end{pmatrix} b_{\mu\gamma} \cdot \frac{\partial}{\partial P} + \mathcal{O}(\delta^2) \tag{53}$$

Using the momentum-jump approximation as described in the text for the two-level system, this expression may be written as

$$\mathrm{e}^{-(J^{(l)}_{1,2\times2}+J^{(l)}_{2,2\times2})\delta} \approx \begin{pmatrix} \cos(a_{\mu\gamma}) & -\sin(a_{\mu\gamma})\hat{j}_{\gamma\mu} \\ \sin(a_{\mu\gamma})\hat{j}_{\mu\gamma} & \cos(a_{\mu\gamma}) \end{pmatrix} + \mathcal{O}(\delta^2) \tag{54}$$

This analysis allows the $\mathcal{N}$-state case to be treated in a manner that is similar to that for a two-level system. Each of the nonadiabatic propagators corresponding to the $\mathcal{J}^{(l)}$ nonadiabatic transition operators is written in a representation $\{s^{(l)}\}$ of states which makes $\mathcal{J}^{(l)}$ block diagonal. The states $|s^{(l)}\rangle$ are simply permutations of the $|s\rangle$ states, $|s^{(l)}\rangle = \mathcal{P}|s\rangle$. These results allow the nonadiabatic propagator for an $\mathcal{N}$-level system to be constructed analytically. The sequence of matrix nonadiabatic propagators may then be sampled using the Monte Carlo method discussed in the text to account for all possible transitions in the manifold of $\mathcal{N}$ states.

References and Notes

(1) Burghardt, I.; Cederbaum, L. S.; Hynes, J. T. *Comput. Phys. Commun.* **2005**, *169*, 95.
(2) Rey, R.; Moller, K. B.; Hynes, J. T. *Chem. Rev.* **2004**, *104*, 1915.
(3) Tully, J. C. *J. Chem. Phys.* **1990**, *93*, 1061.
(4) Hammes-Schiffer, S.; Tully, J. C. *J. Chem. Phys.* **1994**, *101*, 4657.
(5) Xiao, L.; Coker, D. F. *J. Chem. Phys.* **1994**, *100*, 8646.
(6) Webster, F.; Wang, E. T.; Rossky, P. J.; Friesner, R. A. *J. Chem. Phys.* **1994**, *100*, 4835.
(7) Thoss, M.; Wang, H.; Miller, W. H. *J. Chem. Phys.* **2001**, *114*, 9220.
(8) Thompson, K.; Makri, N. *J. Chem. Phys.* **1999**, *110*, 1343.
(9) Makri, N. *J. Phys. Chem. B* **1999**, *103*, 2823.
(10) Shi, Q.; Geva, E. *J. Chem. Phys.* **2004**, *121*, 3393.
(11) Jasper, A. W.; Stechmann, S. N.; Truhlar, D. G. *J. Chem. Phys.* **2002**, *116*, 5424.
(12) Bittner, E.; Schwartz, B. J.; Rossky, P. J. *J. Mol. Struct. THEOCHEM* **1997**, *389*, 203.
(13) Thorndyke, B.; Micha, D. A. *Chem. Phys. Lett.* **2005**, *403*, 280.
(14) Bonella, S.; Coker, D. F. *J. Chem. Phys.* **2005**, *122*, 194102.
(15) Burghardt, I. *J. Chem. Phys.* **2005**, *122*, 094103.
(16) Stock, G.; Thoss, M. *Adv. Chem. Phys.* **2005**, *131*, 243.
(17) Kapral, R.; Ciccotti, G. A Statistical Mechanical Theory of Quantum Dynamics in Classical Environments. In *Bridging Time Scales: Molecular Simulations for the Next Decade*; Nielaba, P., Mareschal, M., Ciccotti, G., Eds.; Springer: Berlin, 2002; p 445.
(18) Kapral, R.; Ciccotti, G. *J. Chem. Phys.* **1999**, *110*, 8919.
(19) Wigner, E. *Phys. Rev.* **1932**, *40*, 749.
(20) Nielsen, S.; Kapral, R.; Ciccotti, G *J. Chem. Phys.* **2001**, 114, 5805.
(21) Kim, H.; Kapral, R. *J. Chem. Phys.* **2005**, *122*, 214105.
(22) Tully, J. C. Mixed quantum-classical dynamics: mean-field and surface-hopping. In *Classical and Quantum Dynamics in Condensed Phase Simulations*, Berne, B. J., Ciccotti, G., Coker, D. F., Eds.; World Scientific: Singapore, 1998; Chapter 21.
(23) Kapral, R. *Annu. Rev. Phys. Chem.* **2006**, *57*, 129.
(24) Mac Kernan, D.; Ciccotti, G.; Kapral, R. *J. Chem. Phys.* **2002**, *116*, 2346.
(25) Aleksandrov, I. V. *Z. Naturforsch. A* **1981**, *36*, 902.
(26) Gerasimenko, V. I. *Theor. Math. Phys.* **1982**, *50*, 49.
(27) Boucher, W. *J. Traschen Phys. Rev. D* **1988**, *37*, 3522.
(28) Zhang, W. Y.; Balescu, R. *J. Plasma Phys.* **1988**, *40*, 199.
(29) Donoso, A.; Martens, C. C. *J. Phys. Chem.* **1998**, *102*, 4291.
(30) Horenko, I.; Salzmann, C.; Schmidt, B.; Schütte, C. *J. Chem. Phys.* **2002**, *117*, 11075.
(31) Santer, M.; Manthe, U.; Stock, G. *J. Chem. Phys.* **2001**, *114*, 2001.
(32) Wan, C.; Schofield, J. *J. Chem. Phys.* **2000**, *113*, 7047.
(33) Nielsen, S.; Kapral, R.; Ciccotti, G. *J. Chem. Phys.* **2000**, *112*, 6543.
(34) Mac Kernan, D.; Kapral, R.; Ciccotti, G. *J. Phys.: Condens. Matter* **2002**, *14*, 9069.
(35) Sergi, A.; Mac Kernan, D.; Ciccotti, G.; Kapral, R. *Theor. Chem. Acc.* **2003**, *110*, 49.
(36) In order to avoid a branching tree of trajectories, which would make the algorithm intractable, the matrix Q_2 in eq 17 must be expanded to second order in δ. Consequently, a third order approximation to the nonadiabatic propagator in eq 19 would not add precision to the algorithm.
(37) A variant of the filter was used in the calculation of proton transfer rates using quantum-classical Liouville dynamics in Hanna, G.; Kapral, R. *J. Chem. Phys.* **2005**, *122*, 244505.
(38) Leggett, A. J.; Chakravarty, Dorsey, A. T.; Fisher, M. P. A.; Garg, A.; Zwerger, M. *Rev. Mod. Phys.* **1987**, *59*, 1.
(39) Weiss, U. *Quantum Dissipative Systems*; World Scientific: Singapore, 1999.
(40) Makarov, D. E.; Makri, N. *Chem. Phys. Lett.* **1994**, *221*, 482.
(41) Egger, R.; Mak, C. H. *J. Phys. Rev. B* **1994**, *50*, 15210.
(42) Golosov, A. A.; Reichman, D. R. *J. Chem. Phys.* **2001**, *114*, 1065.
(43) Mak, C. H.; Chandler, D. *Phys. Rev. A* **1991**, *44*, 2352.
(44) Sun, X.; Wang, H.; Miller, W. H. *J. Chem. Phys.* **1998**, *109*, 7064.
(45) Hanna, G.; Kapral, R. *Acc. Chem. Res.* **2005**, *39*, 21.
(46) Kim, H.; Kapral, R. *J. Chem. Phys.* **2006**, *125*, 234309.